LABORATORY MEASUREMENTS OF WAVE FORCES ON HEAVILY OVERTOPPED VERTICAL WALL

Steven A. Hughes[1], David L. Kriebel[2], Harley S. Winer[3], Edward R. Blodgett[4], and William C. Seabergh[5]

Laboratory experiments were conducted to measure irregular wave forces on a 1:50-scale model of a heavily overtopped thinned-wall vertical current deflection dike located at the mouth of the Mississippi River. The distribution of shoreward-directed peak forces is well represented by the Rayleigh Distribution. Laboratory measurements provided design values for a new structure, and generic design guidance was developed for estimating the root-mean-squared shoreward-directed peak total force and associated moment arm in terms of the incident wave momentum flux and relative wall height. Force estimates using an eigenfuction analysis underestimated the total peak force indicating that flow separation at the top of the submerged wall contributes an additional force that needs to be taken into account in the eigenfunction methodology.

INTRODUCTION AND BACKGROUND

This study provided design values for a vertical, thin-wall dike located at the mouth of the Southwest Pass channel of the Mississippi River in Louisiana, USA. Figure 1 shows the configuration with the dike extending perpendicular from the west river jetty approximately 800 ft (245 m) into the river to divert river flow toward the main navigation channel.

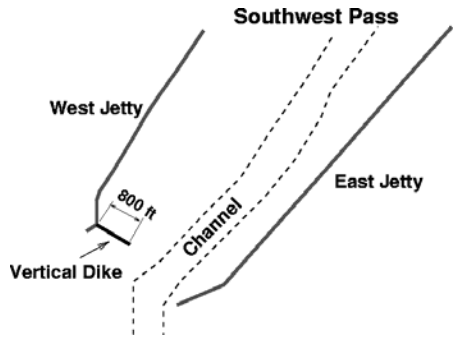

Figure 1. Vertical current deflection dike at mouth of Mississippi River.

[1] Coastal and Hydraulics Laboratory, 3909 Halls Ferry Road, Vicksburg, MS 39180, USA.
[2] U.S. Naval Academy, 121 Blake Road, Annapolis, MD 21402, USA.
[3] New Orleans District, Corps of Engineers, 7400 Leake Ave., New Orleans, LA , USA.
[4] New Orleans District, Corps of Engineers, 7400 Leake Ave., New Orleans, LA, USA.
[5] Coastal and Hydraulics Laboratory, 3909 Halls Ferry Road, Vicksburg, MS 39180, USA.

Water depths along the dike range up to 21 ft (6.4 m). The recently damaged wooden dike structure is to be replaced with a new steel vertical wall having a top elevation either near or below Gulf mean lower low water (mllw) level. Thus, during storms the wall will be heavily overtopped, with the bulk of the storm wave crests passing over the wall. River currents in the upper few feet of the water column will continue to flow seaward over the wall.

With the dike top elevation comparable to the incident storm wave trough elevation the shoreward-directed overflowing water will cause a region of flow separation and lower pressure on the leeside of the wall (Knott and Mackley 1980). This low pressure will increase the shoreward-directed wave force at the top of the wall. Incoming waveform characteristics will be altered by both the partial wave reflection at the wall, and by the out-flowing river current that will steepen the incident wave crests to some degree. All of these factors make this a complex hydrodynamic problem.

The objectives of this study were (1) to determine force and moment loading on the wall for design of this specific structure, and (2) to develop generic design guidance applicable for similar situations.

EXPERIMENTS

Experiments were conducted at a geometrically undistorted length scale of 1:50 using Froude similarity for waves and forces. Figure 2 shows the model setup in an existing inlet research basin equipped with tidal flow capability. In the model the east jetty did not extend as far seaward as in the prototype.

Key experiment parameters in prototype-scale units were reported in Hughes, et al. (2006) as follows. Water elevation was held constant at +1.8 ft mllw and the seafloor elevation at the wall was –22.0 ft mllw giving a total water depth of 23.8 ft for all experiments. Offshore depth at the plunger-type wavemaker was 52.0 ft. Four wall heights were tested having top elevations of –6 ft, -3 ft, +0 ft, and +3 ft mllw. Top wall elevations relative to still water level were –7.8 ft, -4.8 ft, -1.8 ft, and +1.2 ft, respectively. Irregular wave conditions were near depth-limited breaking at the wall for many of the tests. Zeroth-moment significant wave heights (H_{mo}) varied between 5 ft and 12 ft, and the wave period associated with the peak of the wave spectrum (T_p) varied between 7.0 and 13.5 sec. Experiments were conducted without current and with seaward-flowing average current of 3 and 6 ft/sec (prototype-scale units).

Waves were measured at the six locations shown on Figure 2 using capacitance gauges recording at 20-Hz rate. Incident wave parameters were determined from Gauge 2, located left of the model inlet to avoid wave reflection from the vertical wall. Experiment duration was 360 sec, and the number of waves per experiment varied between 190 and 360, depending on wave period.

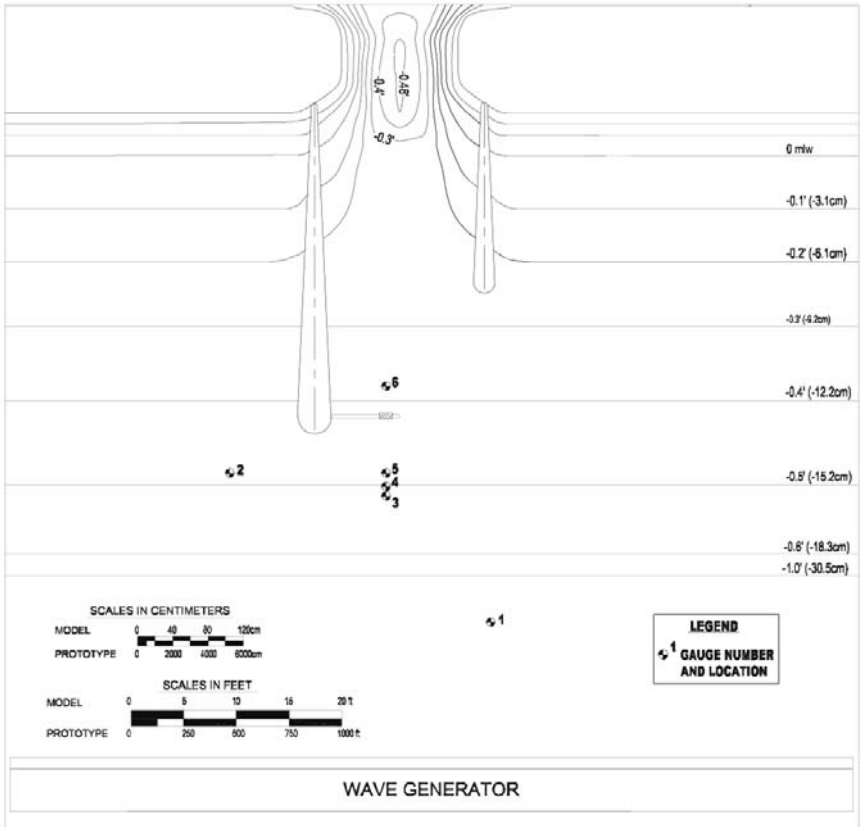

Figure 2. Experiment layout in the generic inlet model basin.

Wave forces on the vertical dike were measured using the apparatus shown in the center photograph in Figure 3. This force-measuring portion is the cantilevered wall section supported by the vertical framework. Narrow gaps separate the supported wall section from the adjacent fixed wall. Wave forces applied over the wall section result in reactions at the upper supports as illustrated by the free-body diagram in Figure 3. Two force transducers were used at the fulcrum point (F_2 and F_3) and a third transducer was used at the top (F_1). Analysis of the free-body diagram at any time yields the total wave force F_L and the corresponding moment arm L_F about the wall base at that instant. Hughes, et al. (2006) discussed calibration of the force-measuring device using the calibration jib shown on the right side of Figure 3, and they estimated a residual moment caused by the rigid connections of the force transducers to the frame so the residual could be removed from experiment force measurements.

Prior to the start of waves for each experiment the load cells were “zeroed” to show no force on the wall. Thus, forces recorded for each experiment

represent the loading due solely to wave motions. Force data were collected from the three load cells at a 40-Hz rate for the same 360-second time period as the wave data. This logging rate was sufficient for recording pulsating wave loads, but the rate was not high enough to record impact loads. Because the top elevation of the wall was well beneath the wave crest elevation, impact loading was much less probable than for emergent walls.

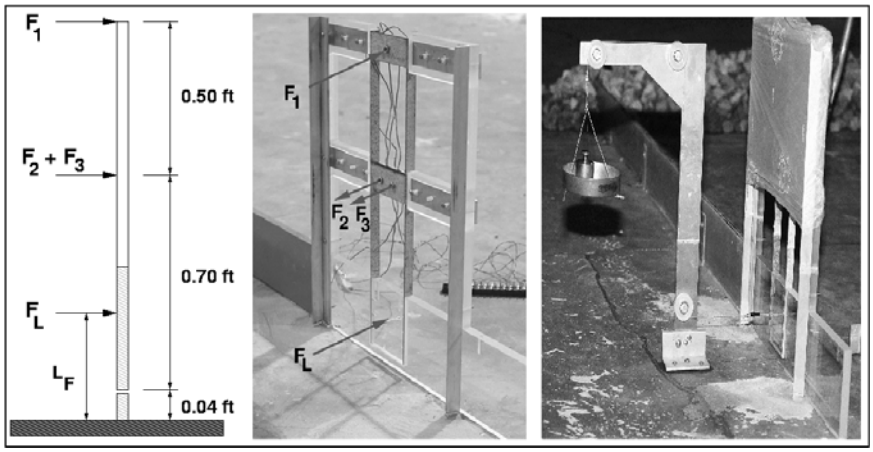

Figure 3. Force measuring wall section (center) and calibration jib (right).

WAVE FORCE ANALYIS

For each experiment the three synchronous force time series were first converted to engineering units (grams) and then combined at each time step according to the force balance equations derived from the free-body diagram of Figure 3. This resulted in time series of the total force on the force-measuring section (F_L) and the corresponding moment arm about the seabed (L_F). The residual moment was included in the moment arm calculation. Model force values were divided by the horizontal width of the force section to give force per unit length, and appropriate scale and conversion factors were applied to yield prototype-scale force per unit length. The force time series exhibited characteristic sharp peaks in the shoreward direction (defined as negative) corresponding to the wave crests, and broad lower peaks in the seaward direction (positive) resulting from the passage of the wave trough over the wall.

The shoreward-directed and seaward-directed peak forces were extracted for each experiment and plotted as distributions normalized by the root-mean-squared of the peak forces (F_{rms}) for the time series. Similarly, the distributions of shoreward- and seaward-directed peak moments were determined as the product of peak force and corresponding moment arm. Forces and moments were always larger in the shoreward direction, and magnitudes increased with

higher wall top elevation, higher zeroth-moment wave height, and longer peak wave periods. The effect of the seaward-directed current only caused a minor reduction in wave force on the vertical wall, and the current effect was not included in subsequent analysis.

Figure 4 shows typical results of the force and moment distributions. The solid curve is the Rayleigh distribution based on the value of F_{rms} for the force peak distributions. For most of the experiments the shoreward-directed peak force distribution was well represented by the Rayleigh distribution whereas the seaward-directed force distribution was a poorer match.

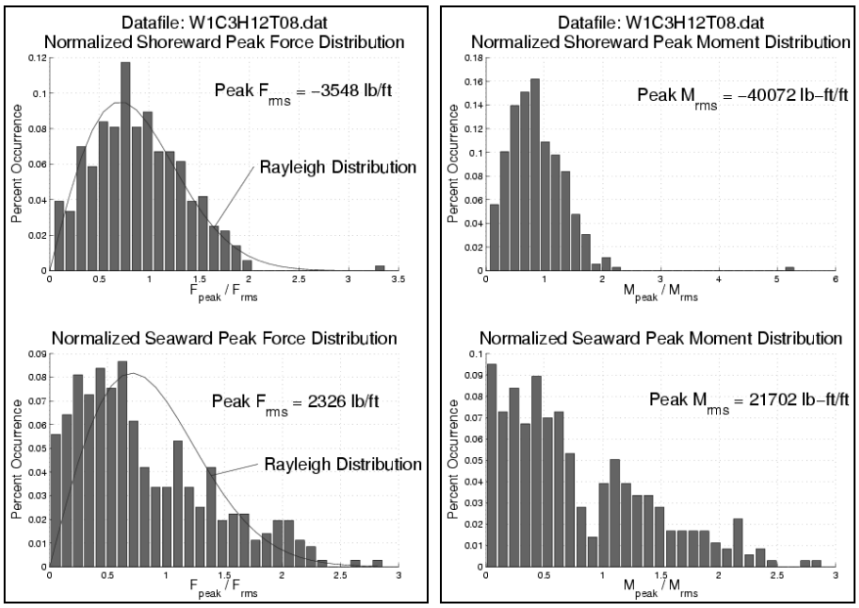

Figure 4. Typical shoreward and seaward force and moment distributions.

The force parameter representing the root-mean-squared values of the shoreward-directed peak forces (in prototype units) is plotted versus the relative depth in Figure 5. Figure 6 shows the variation of $F_{2\%}$ (force that is exceeded by only 2% of the force peaks) that is about twice as large as F_{rms}. Because the water level was constant for all experiments, the abscissa on the Figure 5 plot essentially shows only variation of peak spectral wave period. The peak force parameters increased with higher top wall elevation, increasing wave period (decreasing relative depth), and increasing wave height. Relative wall height appeared to be the most influential test parameter. Most experiments were conducted with waves approaching depth-limited breaking. Tests conducted with lower wave heights introduced additional scatter into the observed trends as seen in Figures 5 and 6 at relative water depth equal to about 0.0078.

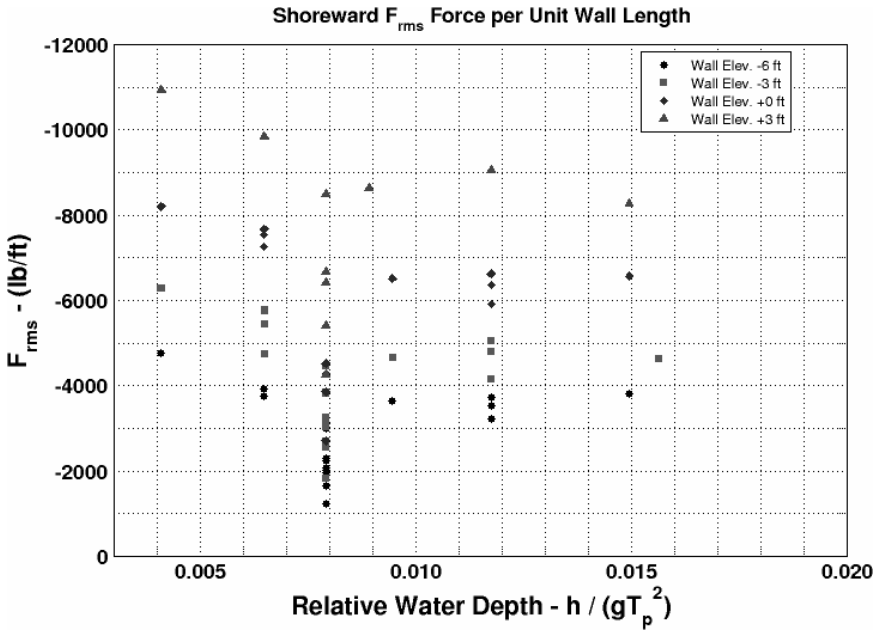

Figure 5. Shoreward-directed root-mean-squared force versus relative depth.

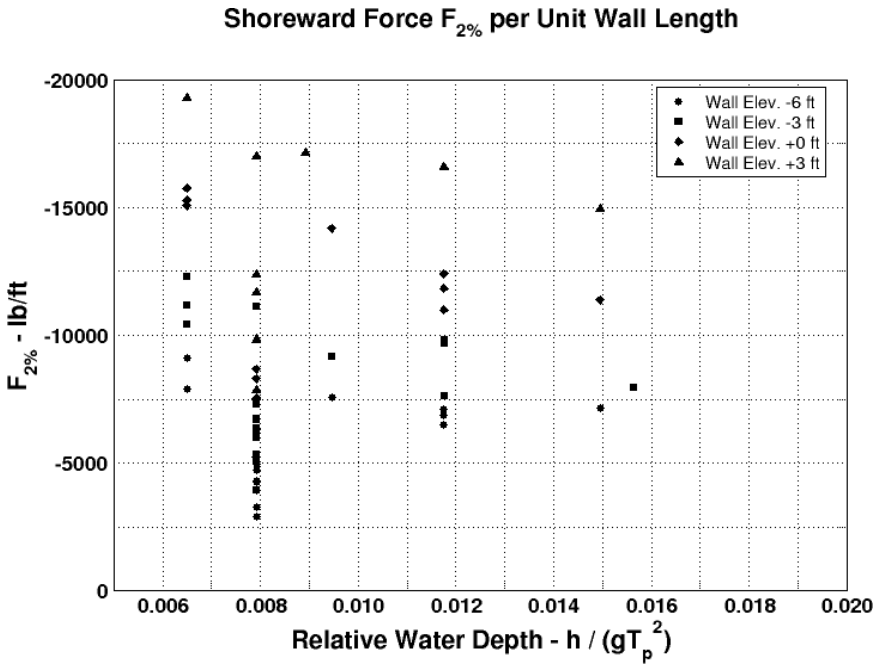

Figure 6. Shoreward-directed 2-percent force versus relative depth.

If the shoreward-directed peak force distribution is well approximated by a Rayleigh distribution based on F_{rms}, estimation methods could focus on correlating F_{rms} to parameters of the incident waves, which is likely to be more successful than correlations based on the extremes of the force distributions. Figure 7 compares actual peak force distribution parameters $F_{1/3}$ (upper plots) and $F_{1/10}$ (lower plots) to estimates using the Rayleigh distribution based on F_{rms} (where $F_{1/3}$ and $F_{1/10}$ are the average of the highest 1/3 and highest 1/10 of the force peaks, respectively).

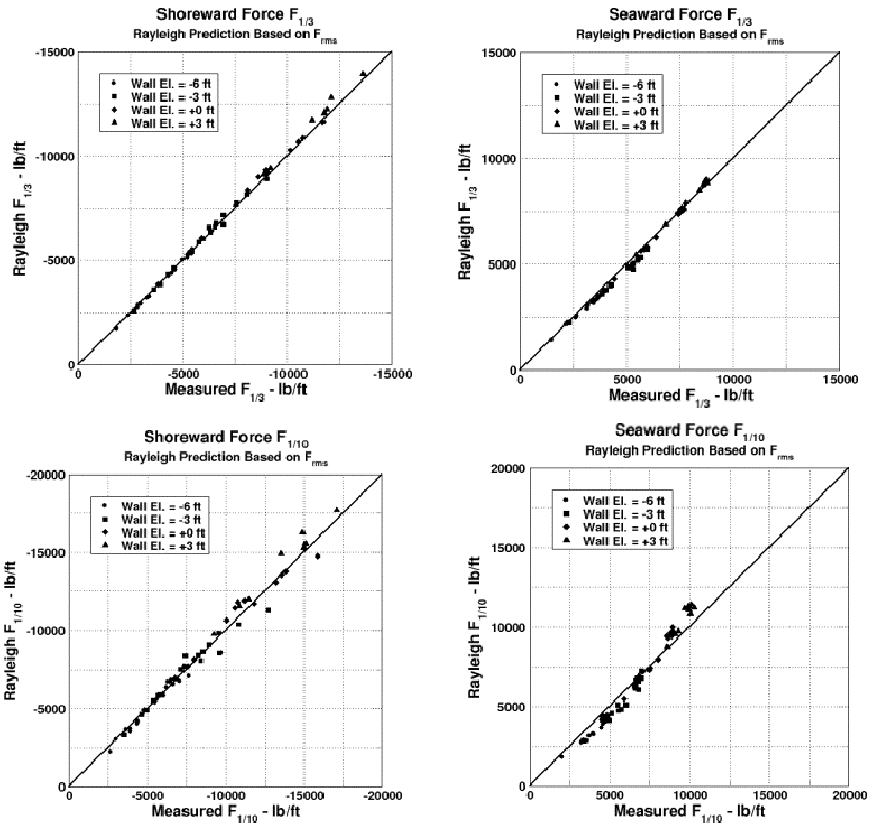

Figure 7. Measurements of $F_{1/3}$ and $F_{1/10}$ compared to Rayleigh predictions.

Rayleigh estimates of $F_{1/3}$ were quite good with little scatter around the line of equivalence. The shoreward-directed forces are slightly better predicted than the seaward-directed forces. More scatter was seen for estimates of $F_{1/10}$ as shown in the lower plots of Figure 7. The scatter for the shoreward-directed forces is not large, and it appears to be evenly distributed about the line of

equivalence. The Rayleigh distribution is less successful for the seaward-directed $F_{1/10}$.

EIGENFUNCTION ANALYSIS

In order to obtain theoretical predictions of the wave forces on a submerged wall, the eigenfunction expansion theory of Kriebel (1999) was adopted with some modifications. The original theory was developed for surface-piercing wave screens that extended from above the water surface down to near mid-depth, leaving a large gap between the bottom of the wall and the seafloor. For the heavily overtopped vertical dike, the wall extends upward from the seafloor, leaving a gap between the top of the wall and the water surface.

The eigenfunction theory is consistent with linear (Airy) wave theory in that it involves solution for the velocity potentials of wave motions on the up-wave (incident wave) and down-wave (transmitted wave) sides of the wall. These up-wave and down-wave solutions must then be appropriately matched at the location of the wall (x=0), to account for the fact that flows can occur above the wall but not through the wall. Thus, both potentials must be zero at the vertical wall boundary, and they must match in the flow region above the top of the wall. A computer solution for the two potentials is determined for a single uniform wave giving an almost exact solution for thin barriers. The potentials then yield the incident, transmitted, and reflected progressive waves, along with the evanescent (or standing wave) modes that exist near the wall[6].

For application to irregular waves, the eigenfunction solution is repeated for each frequency in the incident wave spectrum. Because the eigenfunction solution is consistent with linear wave theory, results from each frequency may then be superimposed to determine the properties of the irregular sea. The eigenfunction analysis does not include any wave breaking at the barrier, and it does not include the steady outflowing river current.

The eigenfunction methodology was applied to the 24 experiments that did not include current, and the ratio of measured peak RMS force to predicted peak RMS force is plotted on Figure 8 as a function of relative water depth. Nearly all the waves cases shown in the figure were depth-limited irregular waves, so in essence, the wave height was constant. The exception are some cases with lower wave heights shown at relative depth equal to about 0.0078.

In nearly all cases the eigenfunction method underestimated the measured forces with errors ranging up to almost 80 percent. The exceptions are cases with a lower wave height and tests with the highest walls.

---

[6] Mathematical details for the original application to wave screens is given in Kriebel (1999). Details of the modifications for overtopped vertical walls are not presented here due to paper length restrictions. Please contact the second author for additional information.

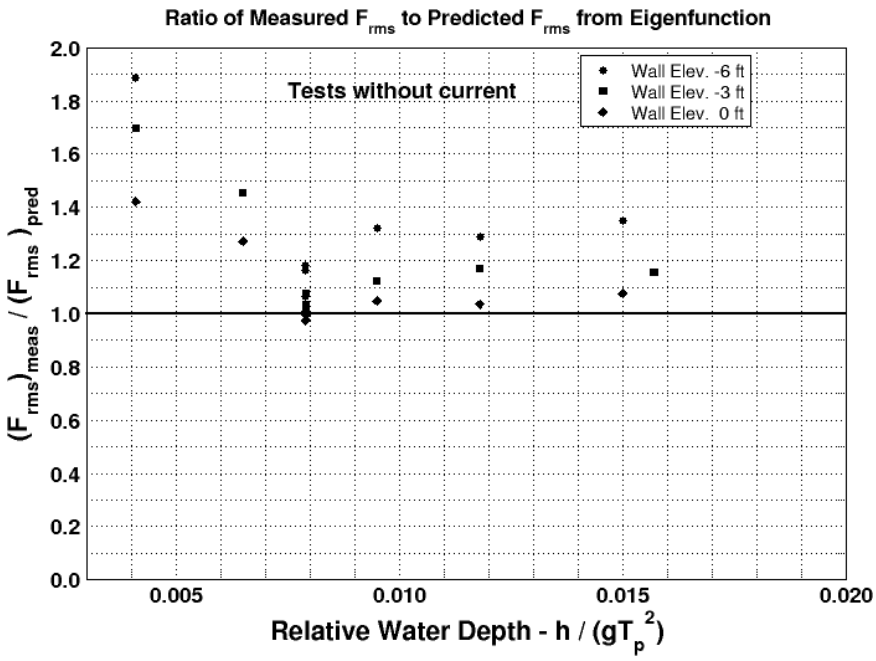

Figure 8. Comparison of Eigenfunction prediction of F_{rms} to measurements.

Figure 8 reveals two likely causes for the discrepancy. First, as the top elevation of the vertical wall becomes more submerged, the eigenfunction method progressively underestimates the actual force. This is thought to be related to flow separation and a low pressure region in the lee of the wall. As more water passes over the wall, the force contribution due to the vortex appears to become larger. However, at some point this increasing trend should taper off as the wall height decreases farther. The shortest wall tested was about 2/3 of the water depth.

The second trend displayed in Figure 8 is the significant increase in the measured-to-predicted force ratio at values of relative depth less than about 0.007. These longer period waves are more nonlinear in form with steep, narrow crests and long, shallow troughs. The nonlinear waves exert a greater force on the wall than linear waves, and the eigenfunction method does not compensate for the non-sinusoidal wave forms. The eigenfunction method needs an additional term to estimate the force related to flow separation at the top of the wall.

EMPIRICAL ANALYIS AND FORCE PREDICTION FORMULAS

Given the complexity of the hydrodynamics and resulting force loading on a heavily overtopped vertical wall, an empirical analysis was used to develop practical design guidance based on the laboratory measurements. The first task was to identify an appropriate normalizing factor for the RMS force that effectively reduces the observed scatter shown on Figure 5 for the range of the experiments. Hughes, et al. (2006) suggested that $F_o / (h_w/h)^2$ might be a good normalizing factor for F_{rms} , where F_o is proportional to some representative total force acting on a fully emergent vertical wall from the bottom to the still water level. Three representations for F_o were considered:

- F_o is proportional to the force on a wall given by linear wave theory
- F_o is proportional to the force on a wall estimated using Goda's (1974) method for forces on walls
- F_o is proportional to the total nonlinear wave momentum flux at the wave crest

Hughes, et al. (2006) noted that force normalization using F_o based on linear wave theory (e.g., Dean and Dalrymple 1984) and calculated using the Goda method resulted in a normalized peak RMS force that still exhibited an increasing trend with increasing wave period. This is probably related to increasing wave nonlinearity that is not captured by the first two methods. However, they found that wave nonlinearity was better represented when F_o was assumed to be proportional to total nonlinear wave momentum flux, M_F as defined by Hughes (2004) by the following formulas

$$\left(\frac{M_F}{\rho g h^2}\right)_{max} = A_0 \left(\frac{h}{gT_p^2}\right)^{-A_1} \tag{1}$$

where

$$A_0 = 0.639 \left(\frac{H_{mo}}{h}\right)^{2.026} \tag{2}$$

$$A_1 = 0.180 \left(\frac{H_{mo}}{h}\right)^{-0.391} \tag{3}$$

and h is water depth, ρ is water density, and g is gravitational acceleration.

Figure 9 presents the shoreward-directed normalized root-mean-squared peak wave force using nonlinear wave momentum flux in the normalizing

factor. The relative wall height parameter accounts for much of the scatter reduction, and the wave momentum flux parameter seems to have accounted for wave nonlinearities because the data no longer exhibit an increase with wave period. The most scatter occurs at the wave period (10 sec prototype) where additional tests were conducted with smaller wave heights. One reason for the scatter could be associated with reduced flow separation as the smaller waves pass over the top of the wall.

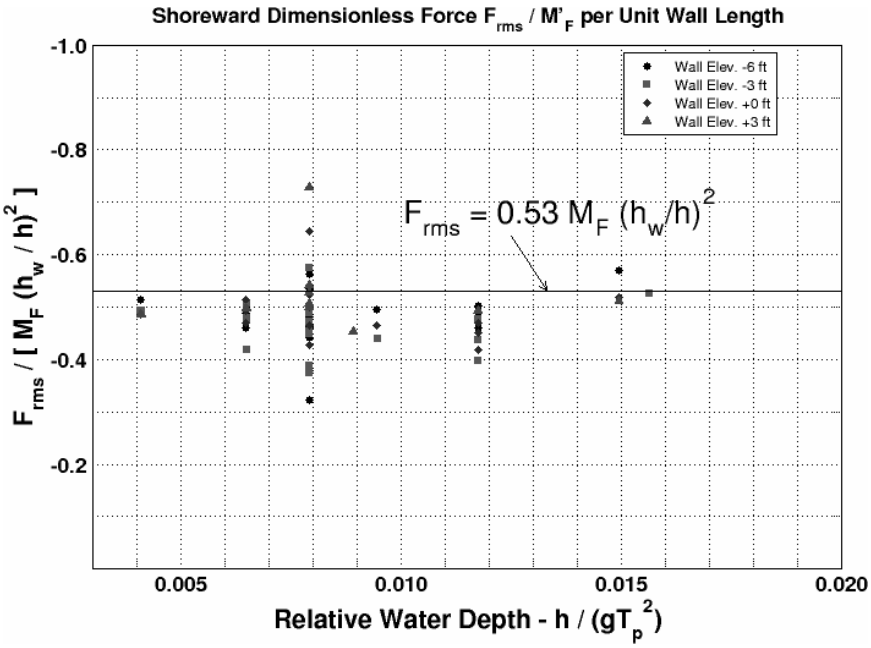

Figure 9. Shoreward-directed normalized root-mean-squared peak force.

The solid horizontal line in Figure 9 was drawn as a conservative recommendation for estimating the shoreward-directed RMS peak wave force acting on the overtopped vertical wall. This resulted in the following simple equation for estimating F_{rms}

$$F_{rms} = 0.53\, M_F \left(\frac{h_w}{h} \right)^2 \tag{4}$$

where M_F is calculated using the formulas given in Eqs. 1-3. Because most of the experiments were conducted with waves approaching the depth-limiting condition, Eq. 4 may not be appropriate for smaller waves in deeper water.

The seaward-directed RMS forces did not show an increasing trend with longer periods indicating wave nonlinearity does not factor into forces related to the wave trough at the vertical wall. For this case, the linear theory approximation for F_o proved adequate as indicated in Figure 10.

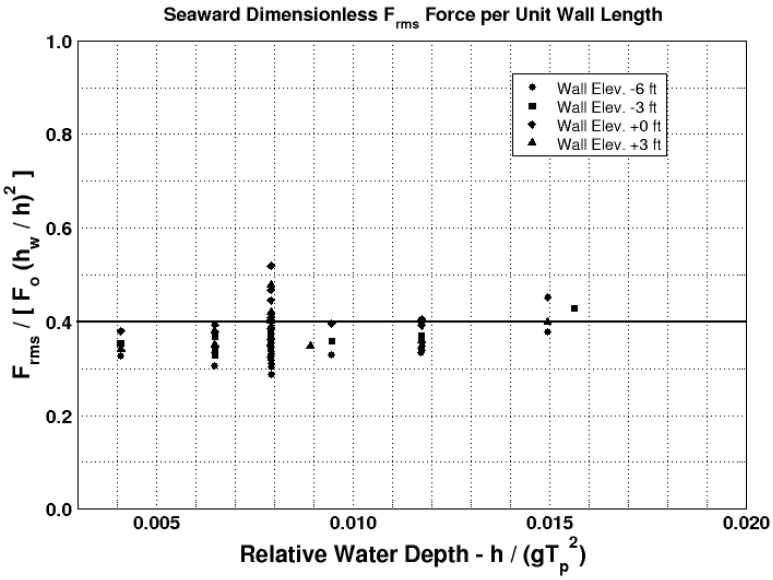

Figure 10. Seaward-directed normalized root-mean-squared peak force.

The solid line in Figure 10 is given by the formula

$$F_{rms} = 0.4\, F_o \left(\frac{h_w}{h} \right)^2 \tag{5}$$

where F_o is given by linear wave theory as

$$F_o = \rho\, g\, H_{mo} \frac{\sinh\left(k_p h \right)}{k_p \cosh\left(k_p h \right)} \tag{6}$$

The moment arm associated with the shoreward-directed RMS force was given by Hughes, et al. (2006) in the form of the strictly empirical equation

$$L_F = 0.4\, h_w \sqrt{\frac{h}{h_w}} \left(\frac{h}{g\, T_p^{\,2}} \right)^{-0.1} \tag{7}$$

which can be multiplied by the representative force to give the corresponding moment of the shoreward-directed force about the bottom of the wall.

SUMMARY

Wave forces on heavily overtopped vertical walls were measured for differing wall heights and wave conditions. The data indicated the distribution of the shoreward-directed force peaks is well represented by the Rayleigh distribution based on the root-mean-squared force. Eigenfunction analysis of the wall underestimated total force because it does not account for flow separation at the top of the wall. An empirical equation was developed to estimate the shoreward-directed RMS peak force. For design application, first estimate the RMS peak force, then use the Rayleigh distribution to obtain an appropriate design force (e.g., $F_{1/100}$), and finally estimate the moment as the product of the force and moment arm given by Eq. 7.

ACKNOWLEDGMENTS

The study described and the results presented herein, unless otherwise noted, were obtained from research funded by the New Orleans District, US Army Corps of Engineers, and by the Coastal Inlets Research Program at the US Army Engineer Research and Development Center. Permission was granted by Headquarters, U.S. Army Corps of Engineers, to publish this information.

REFERENCES

Dean, R. G., and Dalrymple, R. A. 1984. *Water Wave Mechanics for Engineers and Scientists*, Prentice-Hall, Inc., Englewood Cliffs, New Jersey.

Goda, Y. 1974. New wave pressure formulae for composite breakwaters, *Proceedings of the 14th International Coastal Engineering Conference*, ASCE, Vol 3, pp 1702-1720.

Hughes, S. A. 2004. Wave momentum flux parameter: a descriptor for nearshore waves, *Coastal Engineering*, Vol 51, No. 11, pp 1067-1084.

Hughes, S. A., Winer, H. S., and Blodgett, E. R. 2006. Wave forces and moments on heavily overtopped vertical current deflection dike, *Proceedings 1st Intl. Conf. on Application of Physical Modelling to Port and Coastal Protection*, (in publication).

Knott, G. F., and Mackley, M. R. 1980. On eddy motions near plates and ducts induced by water waves and periodic flows, Phil. Trans. of the Royal Society, Vol 294, pp 599-628.

Kriebel, D. L. 1999. Performance of vertical wave barriers in random seas, *Proceedings of Coastal Structures '99*, Balkema, Vol 1, pp 525-532.

KEYWORDS – ICCE 2006

LABORATORY MEASUREMENTS OF WAVE FORCES ON HEAVILY OVERTOPPED VERTICAL WALL

Steven A. Hughes
David L. Kriebel
Harley S. Winer
Edward R. Blodgett
William C. Seabergh

Abstract number 1097

Physical modeling
Coastal structures
Wave forces
Overturning moments
Vertical walls
Wave overtopping
Force distribution
Eigenfunction analysis